Belt Tactile Interface for Communication with Mobile Robot allowing Intelligent Obstacle Detection

Dzmitry Tsetserukou[1,2], Junichi Sugiyama[2] and Jun Miura[2]

[1]EIIRIS, [2]Toyohashi University of Technology

ABSTRACT

This paper focuses on the construction of a novel belt tactile interface and telepresence system intended for mobile robot control. The robotic system consists of a mobile robot and a wearable master robot. The elaborated algorithms allow the robot to precisely recognize the shape, boundaries, movement direction, speed, and distance to the obstacle by means of the laser range finders. The designed tactile belt interface receives the detected information and maps it through the vibrotactile patterns. We designed the patterns in such a way that they convey the obstacle parameters in a very intuitive, robust, and unobtrusive manner. The robot movement direction and speed are governed by the tilt of the user's torso. The sensors embedded into the belt interface measure the user orientation and gestures precisely. Such an interface lets to deeply engage the user into the teleoperation process and to deliver them the tactile perception of the remote environment at the same time. The key point is that the user gets the opportunity to use own arms, hands, fingers for operation of the robotic manipulators and another devices installed on the mobile robot platform. The experimental results of user study revealed the effectiveness of the designed vibration patterns for obstacle parameter presentation. The accuracy in 100% for detection of the moving object by participants was achieved. We believe that the developed robotic system has significant potential in facilitating the navigation of mobile robot while providing a high degree of immersion into remote space.

KEYWORDS: Tactile display, tactile interface, telepresence, mobile robot, proprioception, navigation controller.

INDEX TERMS: H.5.2 [Information interfaces and presentation]: User Interfaces – Haptic I/O, Interaction styles, Prototyping; I.2.9 [Computing Method] Robotics – Operator Interfaces

1 INTRODUCTION

Telepresence robotic system allows a person to feel as if they were present at a place other than their true location [1]. The sense of presence is provided with such stimuli as vision, hearing, sense of touch, etc. [2]. The user of such system is capable of affecting the remote location, and hence, the user position and actions must be sensed and transmitted to the remote robot (teleoperation). As the communication platform, telepresence robot also lets the remote workers to collaborate with others in such an efficient and flexible manner that teleconferencing systems could never permit.

The technical innovations in industry allowed bringing to the market such robotic systems as Anybots QB, Rovio, VGO [3]. The most recent example is the waist-high robot Jazz, which a user can control through web-based interface remotely [4].

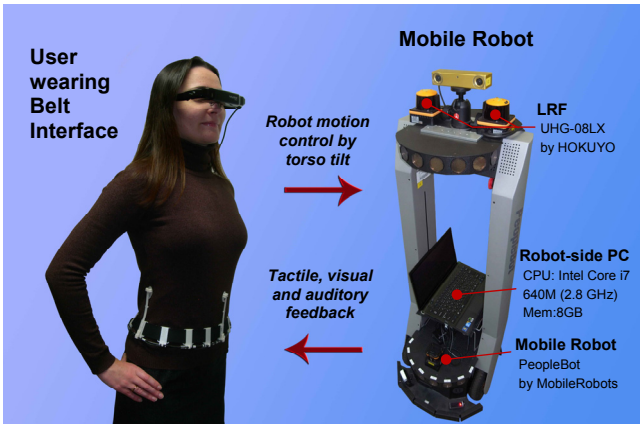

Figure 1. Telepresence robotic system

There is a substantial need in telerobotic interface that allows intuitive and immersive control of the robot. The commonly used interfaces (joystick, keyboard, mouse, PHANTOM) provide a simple but rather not immersive navigation of a planar robot movement [5]. In this case, the human hand is engaged in teleoperation of the remote robot and cannot be used for directing the robotic arm, hand, and fingers of the manipulator mounted on the mobile platform. The purpose of our work is to develop a new type of tactile interface that can make the operator of being "embodied".

The factors that affect the level of immersion are the type of visual facilities (monitor, virtual-reality goggles), auditory feedback, and haptic perception of the remote environment. The novelty of our idea is to engage the user into teleoperation and provide a high level of immersion through proprioseptive telepresence and tactile feedback. That is, the developed interface allows the operator to use their body posture and gestures for controlling the mobile robot and at the same time to feel the remote object through tactile stimuli. The interface augments the remote space perception to the full 360° range around the user via tactile channel (the head mounted display has limited field of view). Thus, the human operator can fully devote the visual faculties to the accomplishment of foreground task.

The important requirement for the telepresence system is to provide the safe interaction of the mobile robot with the remote environment. So, the key point for mobile robot is to accurately detect the obstacle and provide the awareness of the surrounding objects to the human telepresence operator. Therefore, our second research goal is to develop the algorithm and software which can handle the boundaries, distance to obstacles, and mobility (velocity and direction).

In camera-based teleoperation system, two stereo-cameras provide the vision of the remote environment. However, there are several crucial limitations. The narrow view-angle camera cannot

1-1 Hibariga-Oka, Tenpaku-Cho, Toyohashi, Aichi, 441-8581 Japan Email: tsetserukou@eiiris.tut.ac.jp, sugiyama@tut.jp, jun.miura@tut.jp

IEEE World Haptics Conference 2011
21-24 June, Istanbul, Turkey
978-1-4577-0297-6/11/$26.00 ©2011 IEEE

monitor the shadowed and curved areas. Furthermore, when scattered obstacles and, especially, mobile objects (human, other robots, etc.) surround the mobile robot, the operator is unable to handle both the navigation and obstacle recognition. Therefore, we use LRF sensor in order to ensure reliable navigation. Two sensors that are placed on the mobile robot shoulders scan the total 360 degrees. They allow the measurement of the distance to the obstacle and virtual collision vector.

The developed telepresence robotic system comprises the wearable master interface worn on a human body and mobile robot facilitated with sensors (Fig. 1).

2 Telepresence System for Mobile Robot Control

2.1 Principle and Architecture of Telepresence Robotic System

Human operator is capable of changing the robot traveling direction in a smooth and natural manner by twisting and bending the trunk (Fig. 2). The bending flex sensor changes in resistance depending on the amount of the sensor bend. For example, to move the robot forward or backward, the user leans the torso slightly forward or backward, correspondingly. The velocity of the robot is congruent with the trunk tilt angle. When the operator straightens up, the robot stops smoothly. Such operations can allow the human to experience a sense of absolute, natural, instinctive, and safe control.

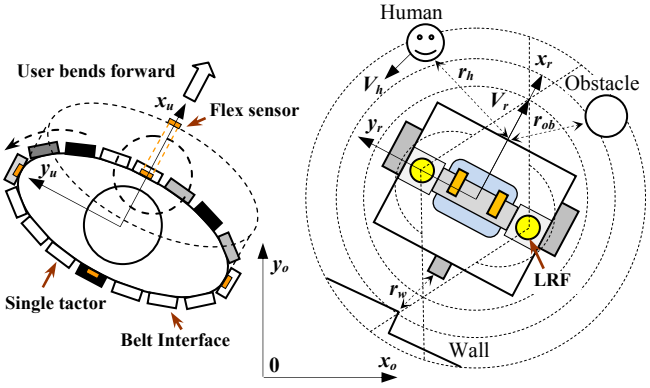

(a) Human operator (b) Mobile robot PeopleBot

Figure 2. Operator-Robot interaction. The colour of the tactor represents the vibration intensity

The developed algorithm analyses the information about the environment and sends it to the wearable master robot. For example, when the detected obstacle is located on the right side of the robot, the user feels the vibration of the tactor at the right side. The belt interface provides the wearer with high resolution vibrotactile signals. Thus, it can also indicate the shape and speed of the object. For example, the convex obstacle is presented by simultaneous activation of three tactors, but with different vibration intensities. The vibration frequency in the middle tactor is larger than in neighboring ones (Fig. 2(a)). The mobile object is represented by the tactile stimuli moving along the waist in the direction of the object travelling (Fig. 2(a)).

The tactile display is connected to the Motor Driver Unit controlled by the signals from the D/A board (Fig. 3). Robot cameras provide the visual feedback from the environment.

2.2 LRF Data Processing

The mobile robot senses the remote environment through the laser range finders (LRF). Fig. 5(a) shows an example of the

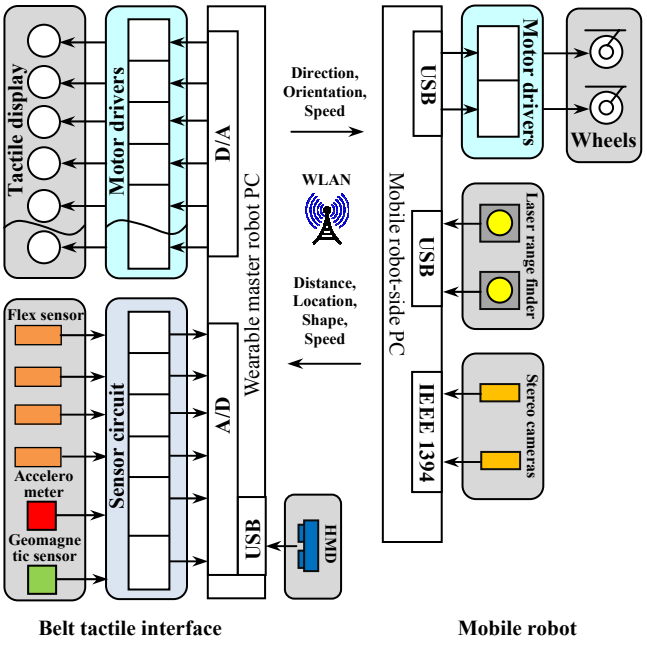

Figure 3. Architecture of the developed telepresence robotic system. The PCs are communicated through the wireless LAN

acquired range data. The data from LRFs are converted into the robot local coordinate to adjust the operator and robot location. The user orientation, sensed by the geomagnetic sensor, corresponds to the planar robot direction.

2.3 Closest Point and Shape Detection

It is very important for the sake of safety to detect the closest obstacles to the robot in the unstructured environment precisely.

In our method, the detection of the closest point and shape is processed by each LRF (measurable range of 8 000 mm, 270°; angular resolution of 0.36°). The nearest obstacle is adopted from the overlapped scan region.

In the detection of the closest point, the distance and the direction of the closest point are extracted from the range data. The detection of the shape around the closest point is conducted though classification of the angle between two vectors connecting the closest point and the point of R apart (see Fig. 4).

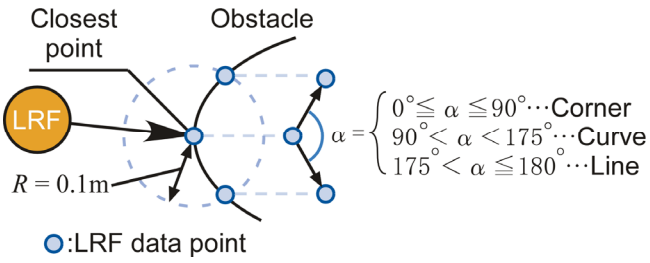

Figure 4. Algorithm for detection of the obstacle shape

The obstacle with the straight border (e.g. wall) is recognized when the 175° < α ≤ 180°. The corner-shaped obstacle has the acute angle between vectors (0° ≤ α ≤ 90°). The obtuse angle (90° ≤ α ≤ 175°) implies that obstacle has a curve profile. Then, the algorithm judges whether arc is convex or concave. If the points of intersections are closer to the robot origin than the closest point, the shape is concave. The opposite statement holds true for the convex profile.

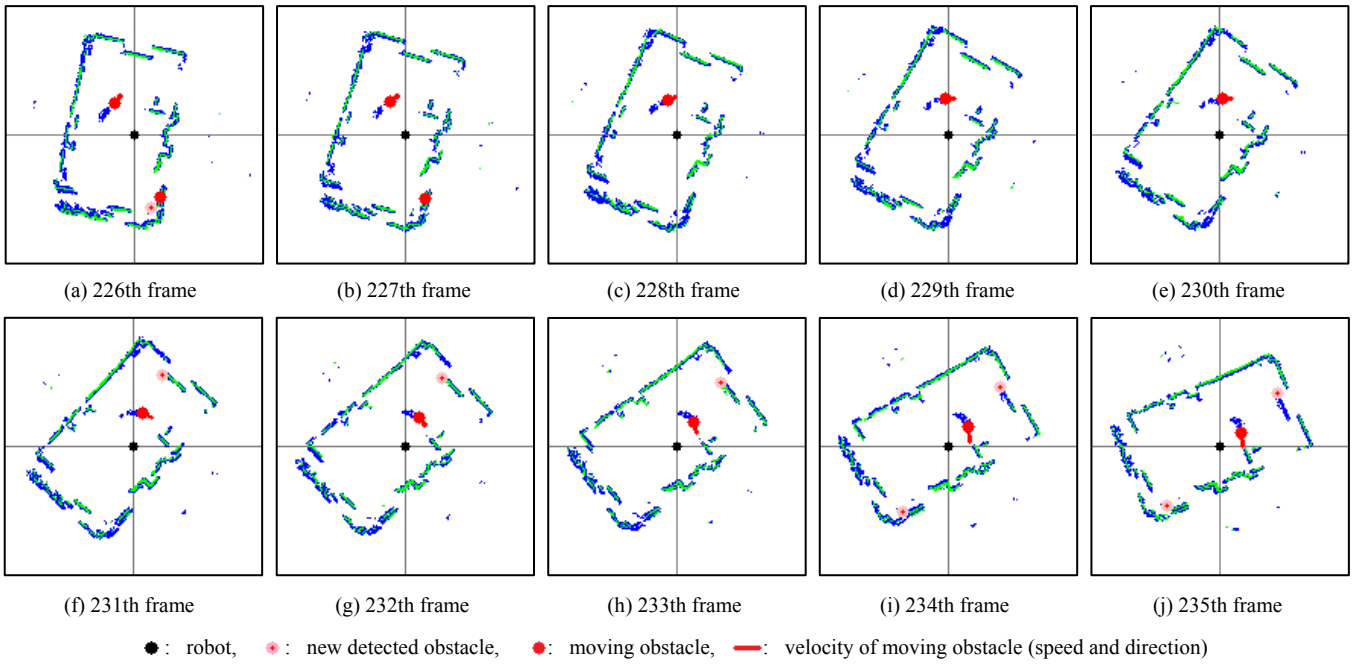

Figure 5. Example of tracking of moving object. The black point on the gray cross depicts the robot location. The white area is the obstacle-free region and the green color lines show the obstacle boundaries. The resolution of the images is 10 pixel/m with the size of 169 x 169 pixels

2.4 Detection and Tracking of the Moving Obstacles

The moving obstacles are considered as more dangerous than the static obstacles in the viewpoint of the fact that they can approach to robot. Several techniques for detection and classification of the moving objects were proposed [6][7]. However, such scan segmentation methods do not work correctly in some cases. Moreover, they cannot deal with the obstacle shape recognition.

In our system, the image converted from the range data of two LRFs (shown in Fig. 6(a)) and robot odometry information are used to detect the moving obstacles and track them. Each moving obstacle is tracked to estimate the state vector x_{Ot} by using Kalman filter (KF):

$$x_{Ot} = \left(p_{Ot}, v_{Ot}\right)^T = \left(p_{xt}, p_{yt}, v_{xt}, v_{yt}\right)^T \quad (1)$$

where $p_{Ot}(p_{xt}, p_{yt})$ is the position of pixel representing the moving obstacle in the range data image; $v_{Ot}(v_{xt}, v_{yt})$ is the velocity of the moving obstacle; t is the time of step.

The following is the procedure of one algorithm cycle.

1. Data acquisition.

First, we acquire the current range data r_t, the robot pose (position and orientation) $p_{Rt}=(x_{Rt}, y_{Rt}, \theta_{Rt})$, and create I_{rt}, the range data image (Fig. 6(a)).

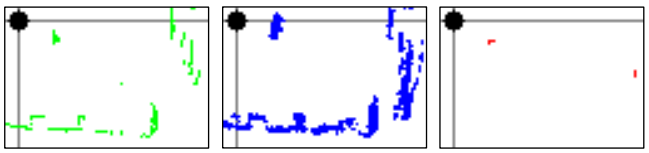

(a) I_{rt} (b) M_t (c) D_t

Figure 6. Detection of moving obstacle

2. Robot pose adjustment based on the history data.

The 8 past frames (this number of stored frames provides high accuracy of moving object detection) of I_{rt-i} (i = 1, 2, ..., 8) are stored. Each past frame is moved with (p_{Rt} - p_{Rt-i}) in eight-neighborhood directions (maximum 8 times) to adjust the pose of the history image to the pose of I_{rt}. The sum of absolute differences indentifies the next image block to be analyzed.

3. Map composition.

We compose the map M_t (Fig. 6(b)) from the eight pose-adjusted history images I_{rt-i} (i = 1, 2, ..., 8) with union operation.

4. Pose adjustment of the obstacles.

The obstacles been tracked are moved at the distance (p_{Rt} - p_{Rt-1}) to adjust the current robot pose.

5. Moving obstacles detection.

M_t is moved on one pixel in eight-neighborhood directions (maximum 8 times) to adjust it to I_{rt}. Then we calculate the difference image I_{rt} - M_t. Difference I_{rt} - M_t includes the pixels existing only in the I_{rt} in order to delete all remaining past trajectories of the moving obstacles. The image of the detected moving obstacles D_t is the relative compliment of M_t in I_{rt}. Each center of mass of the region in the frame D_t is the position of the detected obstacle.

6. Motion prediction (the prediction step of KF).

To estimate the velocity of the moving object from noisy LRF data we employ Kalman filter. For each moving obstacle been tracked, we predict its positions using uniform linear motion model.

7. Data association (observation).

For each predicted obstacle, we calculate the predicted observation.

8. Correction of prediction for obstacles associated with detected ones (update phase of KF).

On this step we calculate the correction step of KF, and gain for the corrected state x_{Ot}.

9. Registration and deletion of the moving obstacles.

The detected obstacles not associated with predicted obstacles are registered and tracked in the next cycle as newly detected obstacle.

10. History update.

Algorithm adds the current data p_{Rt} and I_{rt} into the memory.

Fig. 5(a)-(j) shows the example of the tracking method. In the figure, the green pixels depict I_{rt}, the blue ones - M_t, the red circle and line show the moving obstacle and the velocity. You can see the presence of the miss-detected moving obstacles on the wall. They appear in two cases: (1) insufficient pose adjustment between I_{rt} and M_t, is performed (see Step 2 of the algorithm) and (2) when the part of wall occluded by the moving object becomes visible to the LRF. However, the miss-detected obstacles do not move dramatically, and system disregards them.

3 BELT TACTILE INTERFACE

3.1 Development and Calibration

Wearable tactile display have been shown effective for directional navigation [8][9][10][11][12], assistance to astronauts and pilots orient themselves in environment of degraded afference [13][14], providing signals about body tilt to the persons with balance disorders [15]. It was shown that it was easy and intuitive for subjects to interpret the stimuli location in terms of external direction [16]. User study on vibrotactile way-finding revealed 100% of waypoint accuracy [17][18].

In our research, we employ the tactile stimuli as a modality to deliver the information about the remote environment. The robot is controlled by the user's torso tilt (proprioceptive control). The underlying idea is that while providing the user with tactile awareness of the remote obstacle and intuitive robot navigation, the belt interface allows the operator to devote visual faculties to the exploration of the remote dynamic environment and at the same time to perform manual control of the robot manipulator (e.g., arms, hands, fingers of the robot).

The device is represented by a wearable belt, which is integrated with 16 vibration motors (tactors), four flex sensors, 3-axis accelerometer, geomagnetic sensor, and plastic holders linked by elastic bend (Fig. 7). The proposed structure allows the motor position adjustment for humans of different sizes. The tactors are equally distributed around the user's waist. The motors (operating range of 2.5-3.5 V and corresponding frequency range of 167-250 Hz) vibrate to produce the tactile stimuli indicating the direction, distance, shape, and mobility of the moving obstacle.

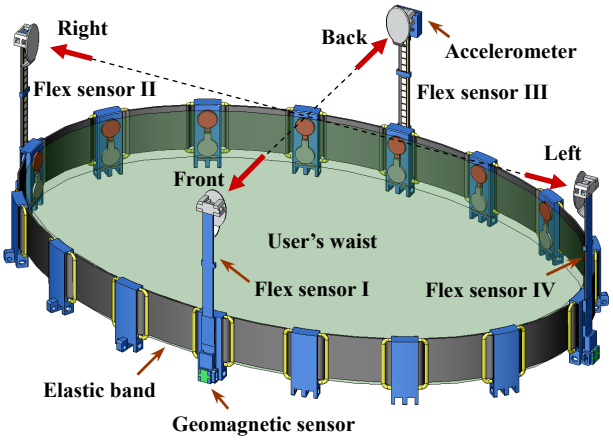

Figure 7. ProInterface aimed at communication with mobile robot. Four Flex sensors (Spectra Symbol 4.5), that contact the user's abdomen, back, and both sides, measure the pose of the torso

The **ProInterafce** (**Pro**prioception-controlled **Interface**) detects the trunk stance through the flex sensors. The 3-axis accelerometer detects the acceleration signal in the vertical direction (Fig. 8). The signal triggers the motion of the robot when user is walking in place (additional method of motion control).

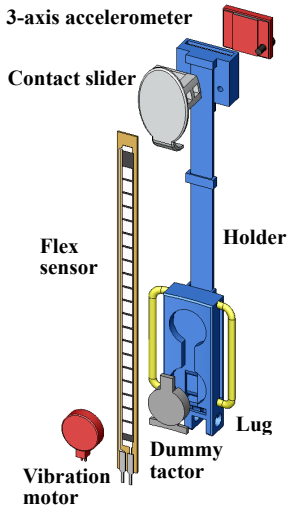

Figure 8. The active unit of the belt

The holder also acts as spring restoring the flex sensor to the initial position. The results of analysis of plastic holder (ABS plastic, force 2 N) using FEM demonstrate the displacement in m (Fig. 9(a)), and von Mises stress $\sigma_{VonMises}$ in N/m^2 (Fig. 9(b)).

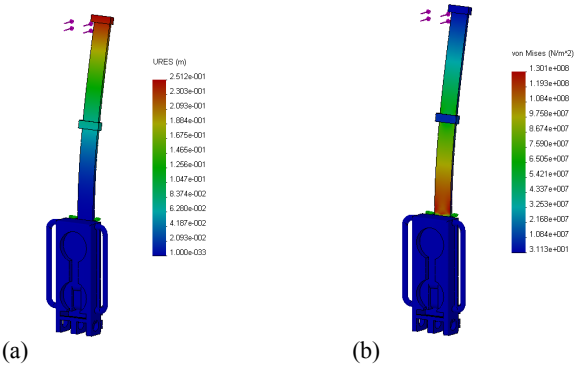

Figure 9. FEM results of the holder spring

During the calibration procedure of flex sensor we simulated the trunk flexion from the neutral trunk position. The base of the holder was fixedly mounted and the tip of the sensor was deflected up to 46 degrees (with the step of 1 degree). The sensor output was recorded on each step. The graph of sensor output voltage vs. trunk angle is relatively linear (Fig. 10).

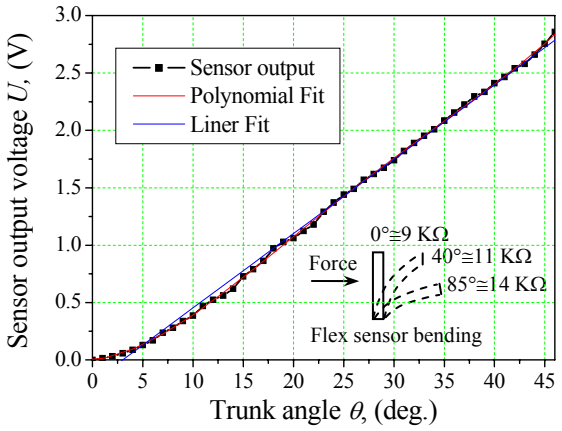

Figure 10. Calibration results of flex sensor

The corresponding equations for lines of best fit with linear and polynomial regression are as follows:

$$y = 0.0648x - 0.195 \ (R^2 = 0.9965) \quad (2)$$

$$y = 9.595 \cdot 10^{-7} x^4 - 1.04x^3 + 0.00388x^2 + \\ +0.01013x - 0.00238 \ (R^2 = 0.9997) \quad (3)$$

The polynomial regression of the calibration data results in a higher coefficient of determination R^2. Based on this evidence, we adopt Eq. (3) for the calculation of the trunk angle.

3.2 Metaphor of Mobile Robot Control

The signals from the flex sensors (U_1, U_2, U_3, U_4) define the coordinates of a logical point $U(x_u, y_u)$:

$$\begin{cases} x_u = \max\{U_1; U_3\} \\ y_u = \max\{U_2; U_4\} \end{cases} \quad (4)$$

The robot changes the linear v and angular velocity ω according to the following equation:

$$\begin{pmatrix} v \\ \omega \end{pmatrix} = \begin{pmatrix} k_v & 0 \\ 0 & k_\omega \end{pmatrix} \begin{pmatrix} R \\ \theta \end{pmatrix} = \begin{pmatrix} k_v & 0 \\ 0 & k_\omega \end{pmatrix} \begin{pmatrix} \sqrt{x_u^2 + y_u^2} \\ \arctan\left(\frac{y_u}{x_u}\right) \end{pmatrix} \quad (5)$$

where k_v and k_ω are the scaling coefficients for the linear and angular speed, correspondingly.

4 User Study Methodology for Belt Interface

The primary purpose of the user study was to evaluate the designed tactile patterns and select those that can convey the tactile information more intuitively and robustly. The developed tactile interface was used to present the shape, and mobility of object.

4.1 Participants

A total of 7 subjects with no previous knowledge about experiment were examined. Their age varied from 24 to 36. The participants were recruited among the students and staff of Toyohashi University of Technology and did not receive any compensation for their participation. None of the subjects reported any sensory difficulties.

4.2 Experimental design. Procedure and Stimuli

The experiment was designed as a within-subjects experiment. In particular, we compare the recognition rates between the vibrotactile stimuli.

Information about obstacle properties is crucial for the operator. Along with the direction of the obstacle location (represented by the location of an active tactor) the shape modality can be delivered as well. The knowledge of the obstacle shape can improve quality of motion planning in unstructured environment. For example, if the Wall is recognized, the operator can navigate the robot along the border.

We designed the tactile patterns for presenting the obstacle shapes in a transparent and intuitive manner. In the pattern recognition experiment, tactors were activated simultaneously with the same impulse duration of 2000 ms. The patterns for presentation of the Corner, Wall, Convex and Concave arc-shaped obstacle, mobile object travelling in Clockwise and Counterclockwise direction relatively the human torso are shown in Fig. 11.

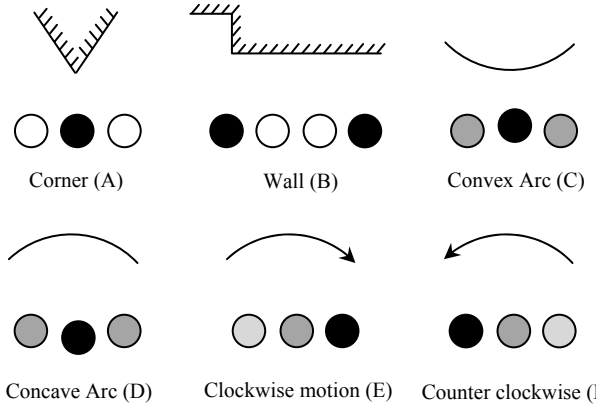

Figure 11. Tactile presentation of the obstacle properties

The notification about detected obstacle with the Corner shape is delivered to the operator through the activation of the single motor. The position of that tactor on the abdomen shows the direction of the obstacle location. To simulate the Wall, two tactors separated by two silent tactors were activated simultaneously. The Convex Arc was presented by activation of all three tactors. The vibration quantity of the middle tactor (250 Hz) was larger than in neighboring ones (188 Hz). Similarly, in the case of Concave Arc the vibration frequency of the outmost tactors (250 Hz) was higher than in middle one (188 Hz). The object moving in the Clockwise direction around the robot body is represented through sequential activation of the tactors in the same direction. Analogously, in the case of Counterclockwise motion the direction of the wave activation is opposite.

4.3 Experimental Procedure

The experiment procedure is as follows. To mask auditory cues of the tactor vibration, subjects wore headphones producing pink noise of 65 dBA. They were asked to wear the belt interface and sit down at the table. The elastic belt embedded in tactile display provided tight contact of motors and torso. Subjects were informed that the experiment aimed at testing their ability to discriminate between various patterns. Additionally, they were shown a diagram of possible patterns of obstacle presentation. All the participants were given 18 trials practice sessions before experiment. They were allowed to look at the visual representation of the patterns at all times of practice session and to identify them.

In total, 60 stimuli (6 patterns were repeated 10 times in a random order) were presented during experiment. The location of the stimuli on the abdomen was randomly selected by software. Thus, the real conditions of communication with robot were simulated. For all patterns, we employed forced methodology. After each stimulus, the subject marked the table cell corresponding to the pattern had been detected. The dependent measure of interest is the recognition rate of the tactile stimulus. The subjects were limited to answer within 10 second. The average duration of four sessions of experiment was 9.5 min.

5 Experimental Results and Discussion.

We conducted a user study in order to evaluate the effectiveness of the developed belt interface. The results of user study are listed

in Table 1. The data are averaged over all subjects. The diagonal term of the confusion matrix indicates the percentage of correct responses of subjects. The mean percentage of the correct answers is 81%.

TABLE 1. GROUP MEAN PERCENTAGE OF RECOGNITION OF OBSTACLE SHAPE AND MOBILITY.

Group Mean Percentage, %	Subject Response					
Actual Pattern	A	B	C	D	E	F
A	**91.4**	0	7.1	1.4	0	0
B	0	**87.1**	4.3	8.6	0	0
C	14.3	5.7	**50.0**	30.0	0	0
D	7.1	11.4	24.3	**57.1**	0	0
E	0	0	0	0	**100.0**	0
F	0	0	0	0	0	**100.0**

As our study involves each subject being measured for each pattern (within-subjects design), in order to see if the differences between Patterns are real or due to chance, we analyze the results of our user study using two-factor ANOVA without replications, with chosen significance level of $p<0.05$. According to the test findings, there is a significant difference in the recognition rates for the different patterns ($F(5,30)=32.4$, $p=0.3\ 10^{-11}<0.05$).

The distinctive pattern for the shape A (a single tactor was activated) resulted in significantly higher recognition rate than the shapes C ($F(1,6)=48.5$, $p=0.00044<0.05$) and D ($F(1,6)=20.82$, $p=0.0038<0.05$). According to ANOVA results, participants recognized pattern B significantly easier than C ($F(1,6)=29.82$, $p=0.0016<0.05$) and D ($F(1,6)=31.5$, $p=0.0014<0.05$).

It was significantly easier for participants to recognize the patterns E and F, representing the moving object, than those representing the shapes A ($F(1,6)=6.35$, $p=0.045<0.05$), B ($F(1,6)=9.35$, $p=0.022<0.05$), C ($F(1,6)=75$, $p=0.00013<0.05$), and D ($F(1,6)=67.5$, $p=0.000175<0.05$). No significant differences were found in recognition rate between other vibration patterns.

The high rates of discrimination of patterns E and F allow the human operator to accurately detect the mobile object and its direction and navigate the remote robot to the safe location. The low recognition rate of the Convex and Concave Arcs (patterns C and D, correspondingly) can be explained by high similarity of vibrotactile stimuli (3 tactors were activated). Therefore, the participants were confused in recognizing them. The possible solution aimed at increasing the discrimination rate is to represent only Convex Arc. The percentages of correct answers for the designed patterns of Corner and Wall demonstrate that such vibrotactile stimuli can be accurately identified and, therefore, could be used for the obstacle presentation to the operator.

6 CONCLUSIONS

We developed a novel wearable, portable, low power, and cost effective belt interface for the communication with mobile robot. The embedded sensors (bend sensor, geomagnetic sensor, and accelerometer) detect the tilt of the operator torso and orientation, thus commanding the speed and direction of the robot. The developed algorithms allow mobile robot equipped with the LRFs to detects the distance, shape and velocity of the object robustly against LRF scan noises.

The sense of tactile telepresence was achieved through vibrotactale stimuli indicating the obstacle presence. We designed the patterns for obstacle properties presentation. The user study on the pattern discrimination shows that participants recognized the moving obstacle and direction with 100% accuracy. The patterns representing the obstacles with Corner and Wall shape also had the high recognition rate (91.4% and 87.1%, respectively).

The developed technology potentially can have a big impact on multi-modal communication with remote robot engaging the user to utilize as many senses as possible, namely, vision, hearing, sense of touch, proprioceprion (posture, gestures). We believe that the telepresence robotic system will result in a high level of immersion into robot space.

The possible applications of the device are mobile robot and vehicle control, navigation of wheel chair, physical therapy, interactive games, etc.

REFERENCES

[1] M. Minsky. Telepresence. *Omni magazine*, 45-51, June 1980.

[2] S. Tachi, Telexistence. World Schientific. Singapore Publishing Co. 2009.

[3] E. Guizzo. When my avatar went to work. *IEEE Spectrum*, 9: 24-30, September 2010

[4] E. Guizzo. Gostai Jazz Telepresence Robot Unveiled. *IEEE Spectrum*, Automation, December 2010, http://spectrum.ieee.org/automaton/robotics/industrial-robots/gostai-jazz-telepresence-robot-unveiled

[5] S. K. Cho, H. Z. Jin, J. Lee, B. Yao. Teleoperation of a mobile robot using a force-reflection joystick with sensing mechanism of rotating magnetic field. *IEEE/ASME Transactions on Mechatronics*, 15(1): 17-26, Feb. 2010.

[6] T. Mori, T. Sato, H. Noguchi, M. Shimosaka, R. Fukui, T. Sato. Moving objects detection and classification based on trajectories of LRF scan data on a grid map. In *Proceedings of IEEE/RSJ IROS '10*, pages 2606-2611, 2010.

[7] J. H. Lee, T. Tubouchi, K. Yamamoto, S. Egawa. People tracking using a robot in motion with laser range finder. In *Proceedings of the IEEE/RSJ IROS '06*, pages 2936-2942, 2006.

[8] K. Tsukada and M. Yasumura. ActiveBelt: belt-type wearable tactile display for directional navigation. In *Proceedings of UBICOMP '04*, pages 384-399, 2004

[9] L. E. M. Grierson, J. Zelek, H. Carnahan. The application of a tactile way-finding belt to facilitate navigation in older person. *Ageing International*, 34(4):203-215, Sept. 2009.

[10] W. Heuten, N. Henze, S. Boll, M. Pielot. Tactile wayfinder: a non-visual support system for way finding. In *Proceedings of NordiCHI '08*, pages 172-181, 2008.

[11] J. R. Marston, J. M. Loomis, R. L. Klatzky, R. G. Golledge. Nonvisual route following with guidance from a simple haptic or auditory display. *Journal of Visual Impairment and Blindness*, 101: 203-211, April 2007.

[12] L. R. Elliot, J. B. F. van Erp, E. S. Redden, M. Duistermaat. Field-based validation of a tactile navigation device. *IEEE Transactions on Haptics*, 3(2):78-87, April-June 2010.

[13] T. Dobbins, S. Samway. The use of tactile navigation cues in high-speed craft operations. In *Proceedings of RINA '02*, pages 13-20, 2002.

[14] H.A.H.C. van Veen, J. B. F. van Erp. Providing directional information with tacile torso displays. In *Proceedings of the Eurohaptics '03*, pages 471-474, 2003.

[15] C. III Wall, M. S. Weinberg, P. B. Schmidt, D. E. Krebs. Balance prosthesis based on micromechanical sensors using vibrotactile feedback of tilt. *IEEE Transactions on Biomedical Engineering*, 48(10):1153-1161, Oct. 2001.

[16] R. W. Cholewiak, J. C. Brill, A. Schwab. Vibrotactile localization on the abdomen: effects of place and space. *Perception and Psychophysics*, 66:970-987, Aug. 2004.

[17] L. A. Jones, B. Lockyer, E. Piateski. Tactile displays and vibrotactile recognition on the torso. *Advanced Robotics*, 20:1359-1374, 2006.

[18] J. B. F. van Erp, H.A.H.C. van Veen, C. Jansen, T. Dobbins. Waypoint navigation with a vibrotactile wais belt. *ACM transactions on Applied Perception*, 2:106-117, 2005.